# Influence of the Adsorbate Structure and Surface Barrier at Micropores. The Adsorption on Columnar-Structured Gold Electrodes of Pyridine from Aqueous Perchlorate Ion-Containing Solutions†

M. M. Gómez,‡ M. P. García,‡ J. San Fabián,‡ L. Vázquez,‡ R. C. Salvarezza,§ and A. J. Arvia*,§

*Departamento de Química-Física Aplicada, C-II, Facultad de Ciencias, Universidad Autónoma de Madrid, 28049 Madrid, Spain, and Instituto de Investigaciones Fisicoquímicas Teóricas y Aplicadas (INIFTA), Sucursal 4, Casilla de Correo 16, (1900) La Plata, Argentina*

*Received October 26, 1995. In Final Form: July 2, 1996*⊗



The electroadsorption on columnar Au electrodes (substrate) of pyridine from $x$ M pyridine + 0.1 M $HClO_4$ and $x$ M pyridine + 0.1 M $KClO_4$ aqueous solutions ($10^{-3} \leq x \leq 10^{-2}$), at constant potential and 298 K, was studied using voltammetry, chronocoulometry, and ac impedance combined with scanning tunneling microscopy to characterize the substrate topography. For a constant pyridine concentration ($c$), the degree of surface coverage by pyridine adsorbate ($\theta$) diminished as $R$ was increased. The $\theta$ vs $c$ plots, irrespective of $R$, were interpreted by a Frumkin adsorption isotherm including a constant standard adsorption free energy. The evaluation of adsorption isotherms reflects the existence of an excluded volume effect, which can be related to a barrier effect due to adsorbates at nanometer size pore entrances.

## 1. Introduction

Molecular adsorption on metal electrodes is strongly influenced by the specific properties of the substrate and has been systematically investigated for the adsorption of pyridine on various metals including single crystals in aqueous environments.[1] It has been demonstrated that, at surfaces of IB elements such as gold single crystals, adsorption is dominated by metal−adsorbate rather than metal−solvent interactions. Furthermore, the surface properties of these metals depend strongly on the surface crystallography. This situation becomes even more complicated when the substrate topography is irregular, as under this circumstance molecular adsorption is affected not only by irregularity in the shape and size distribution but also by adsorbate size and shape. The concept of excluded volume has been introduced to account for these effects.[2]

The influence of topographic features on molecular adsorption can be determined using molecules of different adsorption cross section as yardsticks and adequately selecting solid substrate topographies with reproducible topographic characteristics. It has been recently demonstrated through simulation that heterogeneity in surface geometry is sufficient to induce adsorption/desorption hysteresis loops of different shapes according to the geometry of the surface.[3−5]

The preceding description can be extended to electrochemical interfaces, and in this case, the applied potential also plays a relevant role in determining the stability and configuration of adsorbates, which in turn become potential-dependent adsorbate characteristics. Hence, for molecular adsorption at electrode surfaces, a potential window in which the absence of Faradaic reactions can be assured appears to be most appropriate to examine this complicated problem in a rather simple way.

In the above-mentioned context the adsorption of *o*-phenanthroline has been studied on columnar-structured gold electrodes.[6] The topography of these electrodes approaches that of an irregular surface consisting of columns, deep crevices, and voids[7] which can be described as self-affine surface fractals. These fractals, which exhibit an anisotropic surface disorder, are characterized by a local fractal $D_s$ rather than the fractal dimension characteristic of self-similar (isotropic disordered) fractals.[2] In the case of the stabilized columnar Au electrodes it results in $D_s \cong 2.2$.[7]

Data on *o*-phenanthroline adsorption on this type of gold surface have been interpreted by the existence of an exclusion volume, a concept which is based mainly on the ratio between the yardstick (adsorbate) cross section and the average size of surface irregularities in which the access of the adsorbate is hindered. The excluded volume cross section is given by the difference between the contour of the real substrate and the contour defined by the centers of the adsorbed species on the substrates.[2]

In the case of *o*-phenanthroline adsorption on the columnar gold electrodes, the excluded volume is due to the 1 nm$^2$ molecular cross section and the existence of irregularities of this size in the substrate. However, the excluded volume effect can also be produced by repulsive adsorbate interactions assisted by the irregular topography of the surface. This type of excluded volume seems to be improbable for *o*-phenanthroline adsorption, as it adsorbs flat on the surface and its vertical corrugation is

* To whom correspondence should be addressed.
† Presented at the Second International Symposium on Effects of Surface Heterogeneity in Adsorption and Catalysis on Solids, held in Poland/Slovakia, September 4−10, 1995.
‡ Universidad Autónoma de Madrid.
§ INIFTA.
⊗ Abstract published in *Advance ACS Abstracts,* September 15, 1996.

(1) Lipkowski, J.; Stolberg, L.; Yang, D. F.; Pettinger, B.; Mirwald, S.; Henglein, F.; Kolb, D. M. *Electrochim. Acta* **1994**, *39*, 1045.
(2) Farin, D.; Avnir, D. In *The Fractal Approach to the Heterogeneous Chemistry*; Avnir, D., Ed.; J. Wiley: New York, 1989; p 271. Pfeifer, P.; Obert, M. In *The Fractal Approach to the Heterogeneous Chemistry*; Avnir, D., Ed.; J. Wiley: New York, 1989; p 11.
(3) Seri-Levy, A.; Avnir, D. *Langmuir* **1993**, *9*, 3067; **1993**, *9*, 3073.
(4) Jaroniec, M.; Madey, R. In *Physical Adsorption on Heterogeneous Solids*; Elsevier: Amsterdam, 1988.
(5) Arvia, A. J.; Salvarezza, R. C. *Electrochim. Acta* **1994**, *39*, 1481.
(6) Gómez, M. M.; García, M. P.; San Fabián, J.; Vázquez, L.; Salvarezza, R. C.; Arvia, A. J. Submitted.
(7) Gómez-Rodríguez, J. M.; Vázquez, L.; Baró, A.; Salvarezza, R. C.; Vara, J. M.; Arvia, A. J. *J. Phys. Chem.* **1992**, *96*, 347.

S0743-7463(95)00937-1 CCC: $14.00 

only of the order of 0.1 nm. To explore this possibility, it is interesting to investigate the molecular adsorption of pyridine on the same type of rough gold electrode. In fact, depending on the potential applied to the electrode, the adsorption of pyridine can occur flat or parallel to the substrate, as has been extensively studied on gold single crystals.[1] In the parallel configuration repulsive interactions leading to an excluded volume should occur despite the fact that the pyridine molecule cross section is much smaller than that of *o*-phenanthroline.

In this work, the adsorption of pyridine on columnar-structured gold electrodes was studied by voltammetry, chronocoulometry, and ac impendance. The topography of this type of electrode was characterized by in-situ STM. The electrochemical adsorption isotherms obey a Frumkin-type equation in which an excluded volume correction is incorporated to account for the influence of the gold electrode surface roughness. The dependence of the excluded volume correction on the electrode roughness is consistent with a hindrance to the surface accessibility by pyridine molecules at the smallest voids and crevices. The existence of an excluded volume effect can be related to a barrier effect due to adsorbates at nanometer size pore entrances.

## 2. Experimental Section

Electrochemical runs were performed with a conventional glass-made cell involving a columnar Au working electrode, a large area Au counter electrode, and a $Hg/Hg_2SO_4$ (MSE) reference electrode, $E°$/V (SHE) = 0.650. All potentials given in the text are referred to the MSE scale.

Each columnar Au electrode (*we*) was prepared in situ by means of the electrochemical roughening procedure which has been extensively described elsewhere.[8,9-11] Briefly, a polycrystalline Au wire immersed in 0.5 M $H_2SO_4$ was anodized at 2.0 V for a preset time ($t$) at room temperature to accumulate a certain amount of hydrous Au oxide. Subsequently, the oxide layer was electroreduced by applying a linear potential sweep from 1.0 to −0.6 V at 0.1 V/s. It has been shown[11,12] that the oxide/metal overlayer phase change proceeds under a nearly constant oxide volume condition. Accordingly, the value of $h$, the average thickness of the Au overlayer, could be estimated from

$$h = Mq/zF\rho \qquad (1)$$

where $q$ is the Au oxide electroreduction charge referred to the substrate area, $M = 442$ g mol$^{-1}$ is the molecular weight of the Au oxide, $\rho = 11$ g cm$^{-3}$ is the oxide density, and $z = 6$ is the number of electrons transferred per mole of oxide. The values of $h$ derived from eq 1 agreed with those resulting from the cross-section measurements made on scanning electron microscopy micrographs of columnar Au electrodes.[11,12] Thus, as $q \propto t$, by adjusting $t$ adequately, the average thickness of the columnar Au layer was varied between $1 \times 10^{-6}$ and $1 \times 10^{-3}$ cm. Correspondingly, the value of $R$, the roughness factor, was varied in the range $1 \le R \le 55$.

The value of $R$ was voltammetrically determined from the charge ratio of the O-adatom monolayer electrodesorption at the columnar Au electrode and smooth Au wire electrode.[8] For this purpose voltammograms were run in aqueous 1 M $H_2SO_4$ at 0.1 V s$^{-1}$ between −0.55 and 1.15 V. No roughness factor correction for the smooth Au wire was made, as the corresponding value of $R$ was always between 1.0 and 1.1.

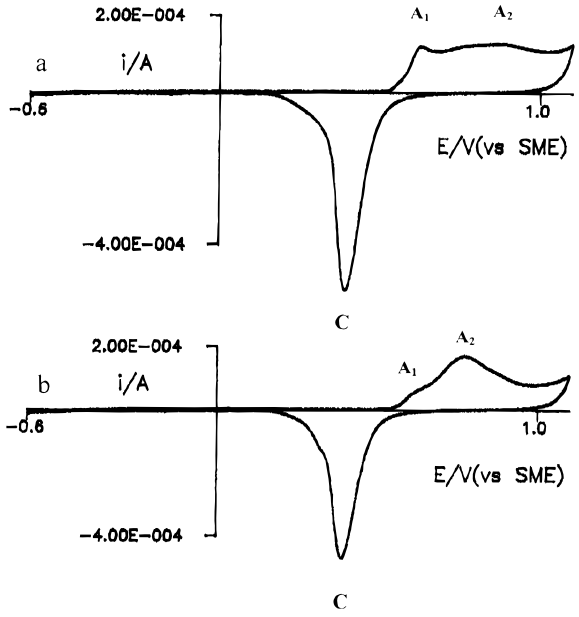


**Figure 1.** Voltammograms of Au electrodes ($R = 25$) in (a) 0.1 M $HClO_4$ and (b) 0.1 M $HClO_4$ + 0.0025 M pyridine run at 0.1 V s$^{-1}$ and 25 °C.

As already reported,[12] columnar Au electrodes exhibit a surface roughness relaxation which extends to about $1 \times 10^5$ s at room temperature, due to the relatively high mobility of Au atoms at the metal/electrolyte interface. To overcome this drawback, only stabilized Au electrodes, i.e. those columnar electrodes which were aged in aqueous 0.5 M $H_2SO_4$ for $10^5$ s, were used in this work. Previous to each adsorption experiment the stabilized Au electrode was cleaned by potential cycling at 0.1 V s$^{-1}$ in 0.5 M $H_2SO_4$ in the range −0.6 to −1.2 V until the well-known voltammetric response of the polycrystalline Au electrode in the same solution was obtained (Figure 1a). Hereafter, stabilized cleaned Au electrodes are denoted as cs-Au electrodes.

Impedance measurements were made in the range 10 Hz ≤ $f$ ≤ 10 KHz with a 10 mV amplitude, where $f = \omega/2\pi$, $\omega$ being the angular velocity. For aqueous 0.1 M $HClO_4$ and aqueous 0.1 M $HClO_4$ + $x$ M pyridine ($0 \le x \le 10^{-2}$), the potential range −0.7 V ≤ $E$ ≤ 0.5 was covered, whereas for aqueous 0.1 M $KClO_4$ and aqueous 0.1 M $KClO_4$ + $x$ M Py ($0 \le x \le 10^{-2}$) runs were made in the range −1.2 V ≤ $E$ ≤ 0.5 V.

Conventional voltammetry was run at 0.1 V s$^{-1}$ in both types of solution covering different values of $E_{sa}$ and $E_{sc}$, the anodic and cathodic switching potential, respectively.

Solutions were prepared from twice distilled water, which was passed through a Millipore-MilliQ* system, and Merck p.a. quality chemicals. Solutions were kept under nitrogen. All runs were performed at 25 °C.

Chronocoulometry was employed to study the adsorption of pyridine on the gold electrode surface. The charge density ($q$) vs applied potential ($E$) plots were obtained in the following way. The *we* was first held for 3 min at $E_c$, a potential sufficiently negative to prevent Py adsorption on the *we*. Thus, for aqueous 0.1 M $HClO_4$ and 0.1 M $KClO_4$ the values $E_c = -0.7$ V and $E_c = -1.2$ V, respectively, were chosen. Subsequently, the potential was stepped from $E_c$ to $E_{ad}$, the potential at which the adsorption of Py took place, i.e., −0.7 V < $E_{ad}$ < 0.4 V and −1.2 V < $E_{ad}$ < 0 V, in aqueous $HClO_4$ and $KClO_4$ solutions, respectively, and simultaneously the current ($I$) vs time ($t$) plot was recorded. A null current value was obtained for $t > 0.1$ s for all electrodes, indicating that pyridine adsorption had been completed for all cs-Au electrodes used in our work. This was demonstrated by experiments made with a cs-Au electrode ($R = 30$) in the range 0.1 s ≤ $t$ ≤ 5 s, in which no difference in $q$ was found. Therefore, for chronocoulometry the value $t = 0.1$ s was set. Then, after Py adsorption for $t = 0.1$ s, the potential was stepped back from $E_{ad}$ to $E_c$ to assist Py desorption from the *we*. Then, for each $E$, the value of $q$ was obtained by integration of the $I$ vs $t$ plot taking into account the real electrode area. The linear portion of the $q$ vs $t$ plot related to the steady state was obtained from extrapolation by linear regression to $t = 0$.

(8) Chialvo, A. C.; Triaca, W. E.; Arvia, A. J. *J. Electroanal. Chem.* **1984**, *171*, 303.
(9) Arvia, A. J.; Salvarezza, R. C. *Electrochim. Acta* **1992**, *37*, 2155.
(10) Chialvo, A. C.; Triaca, W. E.; Arvia, A. J. *J. Electroanal. Chem.* **1983**, *146*, 43.
(11) Vázquez, L.; Bartolomé, A.; Baró, A. M.; Alonso, C.; Salvarezza, R. C.; Arvia, A. J. *Surf. Sci.* **1989**, *215*, 171.
(12) Alonso, C.; Salvarezza, R. C.; Vara, J. M.; Arvia, A. J.; Vázquez, L.; Bartolomé, A.; Baró, A. M. *J. Electrochem. Soc.* **1990**, *137*, 2161.

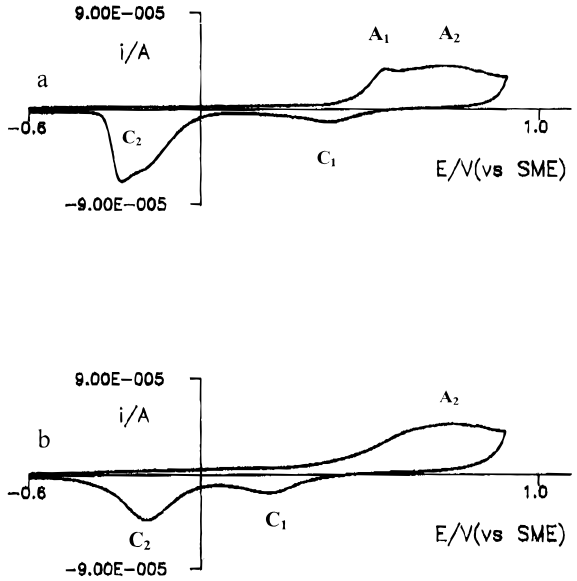


**Figure 2.** Voltammograms of Au electrodes ($R = 9$) in (a) 0.1 M $KClO_4$ and (b) 0.1 M $KClO_4$ + 0.01 M pyridine run at 0.1 V $s^{-1}$ and 25 °C.

In-situ scanning tunneling microscopy images of cs-Au electrodes in aqueous 0.5 M $H_2SO_4$ at $E = 0.1$ V were obtained in the constant current mode, using Nanoscope III equipment (Digital Instruments, Santa Barbara, CA) and Pt-IR Nanotips applying a 0.1 V bias voltage and a 10 nA tunneling current.

## 3. Results and Interpretation

**3.1. Voltammetric Data.** Voltammograms (blanks) resulting from cs-Au (Figure 1a and 2a) and polycrystalline Au electrodes ($R = 1$) at 0.1 V/s in either aqueous 0.1 M $HClO_4$ or aqueous 0.1 M $KClO_4$ exhibit some common features except for a current scale factor. These voltammograms show an anodic current contribution consisting of two peaks, $A_1$ and $A_2$, in the range 0.6−1.1 V for aqueous 0.1 M $HClO_4$ and in the range 0.2−0.7 V for aqueous 0.1 M $KClO_4$. These peaks are related to the formation of the O-containing monolayer on Au. The electroreduction of this monolayer takes place at a lower potential range which depends on the composition of the solution.[13] The $H_2$ evolution reaction on Au in these solutions commences at potentials more negative than −0.7 and −1.2 V for 0.1 M $HClO_4$ and 0.1 M $KClO_4$, respectively. These voltammograms comprise the anodic-to-cathodic charge density ratio $q_a/q_b = 1$ and show a rather wide potential window between −0.7 and ca. 0.5 V for aqueous $HClO_4$ and between −1.2 and 0.1 V for aqueous 0.1 M $KClO_4$ in which Faradaic processes are not observed.

On the other hand, voltammograms run in Py-containing solutions under conditions comparable to those used for the blanks after properly adjusting $E_{sa}$ and $E_{sc}$ (Figures 1b and 2b) show a considerable difference. Thus, in aqueous 0.1 M $HClO_4$ (Figure 1b) the presence of Py shifts the threshold potential for the formation of the O-containing monolayer nearly 0.1 V positively, the resistance of the Faradaic process increases, peak $A_1$ is suppressed, and the value of $q_a$ becomes somewhat lower than that of the blank. Likewise, the electroreduction peak related to the O-containing monolayer moves negatively and $q_b$, the corresponding charge density, decreases.

(13) Ferro, C. M.; Calandra, A. J.; Arvia, A. J. *J. Electroanal. Chem.* **1975**, *59*, 239.

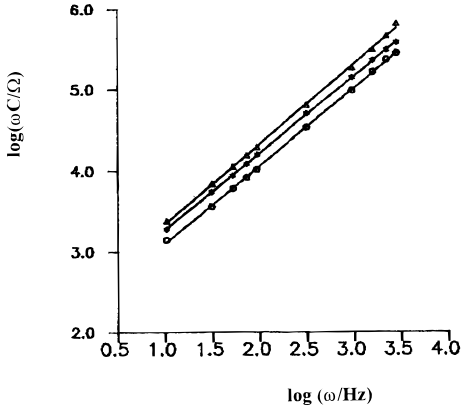


**Figure 3.** Log $\omega C$ vs log $\omega$ plots for cs-Au electrodes ($R = 51$) in aqueous 0.1 M $HClO_4$ + $x$ M Py at 25 °C. (∗) $x = 0.001$, $E = -0.01$ V; (○) $x = 0.01$ M, $E = -0.1$ V; (△) $x = 0.01$, $E = -0.6$ V. The slope of the straight lines in 0.955 ± 0.015.

A similar qualitative description applies to the voltammograms resulting in aqueous Py-containing 0.1 M $KClO_4$ (Figure 2b), although in this case more drastic changes are observed.

In both cases, it appears that, in the range covered by the voltammograms shown in Figures 1b and 2b, there is not significant Faradaic contribution involving Py directly.[14] It seems, therefore, reasonable to attribute the voltammetric changes described above to a partial blockage of the Au electrode surface by pyridine molecular adsorption, producing mainly a hindrance of the O-containing monolayer formation, as has already been reported for some related compounds. It should be noted that by holding the potential at a value chosen within the double-layer region for adsorption times in the range 0.1−60 s the voltammetric charge related to both the O-containing monolayer formation and its corresponding electroreduction remained unchanged. These results can be considered as a first indication that pyridine adsorption on cs-Au electrodes is completed for $t < 0.1$ s.

**3.2. Differential Capacitance Data.** For cs-Au electrodes in the electrolyte solutions used in this work the log $\omega C_d$ vs log $\omega$ plot yields straight lines with a slope 0.955 ± 0.015 (Figure 3), a figure close to that observed for polycrystalline and Au single-crystal electrodes.[15] This means that for cs-Au electrodes in our working solutions the frequency dispersion is not relevant. In fact, as discussed in detail in ref 16, rough electrodes usually exhibit a frequency dispersion of the measured differential capacitance, particularly when diluted solutions are used. However, to avoid an underestimation in the value of $C_d$, measurements were carried out at 10 Hz.

The values of $C_d$, the differential capacitance obtained at 10 Hz and different $E$ values for cs-Au in solutions both with and without Py addition, are shown in Figures 4−6. The values of $C_d$ are referred to the real surface area of the *we*.

The $C_d$ vs $E$ plots resulting from 0.1 M $HClO_4$ (Figure 4, dashed line) exhibit two maxima, $C_{d,II}$ and $C_{d,I}$ at −0.6 and −0.2 V, respectively, irrespective of $R$. The shape of these plots agrees with data reported in the literature for Au.[17] The minimum value of $C_d$ is very close to the potential of zero charge of polycrystalline gold, $E_{pzc} = -0.42$

(14) Stolberg, L.; Richer, J.; Lipkowski, J.; Irish, D. E. *J. Electroanal. Chem.* **1986**, *207*, 213.
(15) Real, S. G.; Vilche, J. R.; Arvia, A. J. *J. Electroanal. Chem.* **1992**, *341*, 181 and references therein.
(16) Gómez, M. M.; Vázquez, L.; Salvarezza, R. C.; Vara, J. M.; Arvia, A. J. *J. Electroanal. Chem.* **1991**, *317*, 125.
(17) Hamelin, A. *J. Electroanal. Chem.* **1988**, *255*, 281.

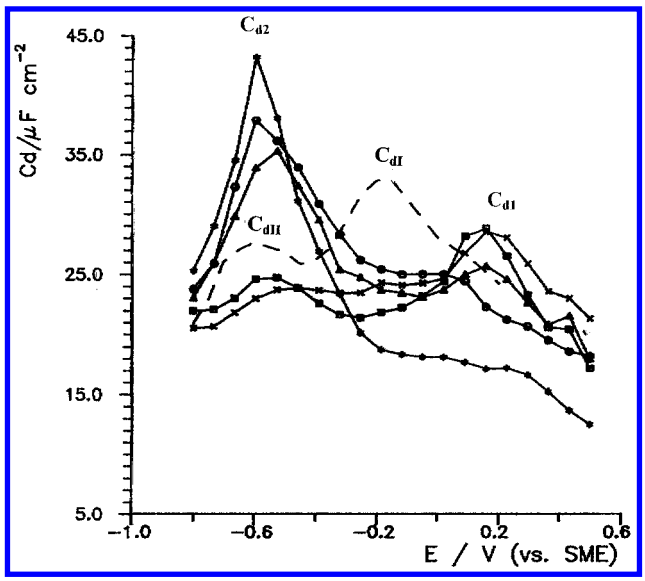


**Figure 4.** $C_d$ vs $E$ plots for Au electrodes ($R = 1$) in 0.1 M $HClO_4$ + $x$ M Py at 25 °C: (dashed line) $x = 0$; (×) $x = 0.001$; (□) $x = 0.0025$; (△) $x = 0.005$; (○) 0.0075; (∗) $x = 0.01$.

V.[18] It might appear that the minimum value of $C_d$ for cs-Au electrodes in 0.1 M $HClO_4$ is casual due to the minimum in the capacitance of the compact part of the electrical double layer. However, measurements made with cs-Au electrodes in 0.01 M $HClO_4$ show that this minimum in the $C_d$ vs $E$ plot coincides with the $E_{pzc}$ value, in agreement with the literature.[18] Therefore, we have considered that for our system it is reasonable to take $E_{pzc} = -0.42$ V.

The electrical double-layer structure in the potential region around $E_{pzc}$ is dominated by the diffuse part of the double layer, whereas the rising portion of the $C_d$ vs $E$ plot at positive potentials defines a maximum value of $C_d$ which can be assigned to the contribution of the inner part of the double layer.[19] At $E > E_{pzc}$ and $E < E_{pzc}$ anion−gold and cation−gold interactions, respectively, play a relevant role in the structure of the electrical double layer. From the integration of the $C_d$ vs $E$ plots the value of $\sigma^s$, the electrode charge density, was obtained. For this purpose $\sigma^s = 0$ at $E = E_{pzc}$ was taken.

The $C_d$ vs $E$ plots resulting from aqueous Py-containing 0.1 M $HClO_4$ solutions exhibit a rather complex behavior (Figures 4 and 5) which depends strongly on the value of $x$ as well as on the value of $R$ and the base electrolyte composition. Thus, for $R = 1$ and $x = 10^{-3}$ (Figure 4), the value of $C_d$ shows two plateaus in the range −0.7 to 0 V followed by the peak value of $C_{d,1} = 25 \pm 2$ μF cm$^{-2}$ at ca. 0.2 V. As $x$ is gradually increased, the $C_d$ vs $E$ plot exhibits a gradual decrease in $C_{d,1}$ and a new gradually increasing peak $C_{d,2}$ at −0.6 V. Finally, for $x = 0.01$, only $C_{d,2}$ can be distinguished, which is followed by a plateau in the range −0.2 to 0 V and its subsequent decrease on further increasing $E$ positively.

The $C_d$ vs $E$ plot resulting from a cs-Au electrode ($R = 29$) under the above-mentioned conditions (Figure 5a) is rather different from that found for $R = 1$. Thus, at the lowest concentration by Py three peak values of $C_d$ are observed, namely, $C_{d,1}$, $C_{d,2}$, and $C_{d,3}$, at 0.2, −0.6, and −0.22 V, respectively. But as the concentration of Py is raised, the height of $C_{d,3}$ gradually disappears and only a large contribution of $C_{d,2}$ and a minor contribution of $C_{d,1}$ can be seen. The potential difference related to $C_{d,1}$ and $C_{d,2}$ is about 0.7 V.

(18) Clavilier, J.; Van Huong, C. N. *J. Electroanal. Chem.* **1977**, *80*, 101.
(19) Payne, R. *J. Phys. Chem.* **1966**, *70*, 204.

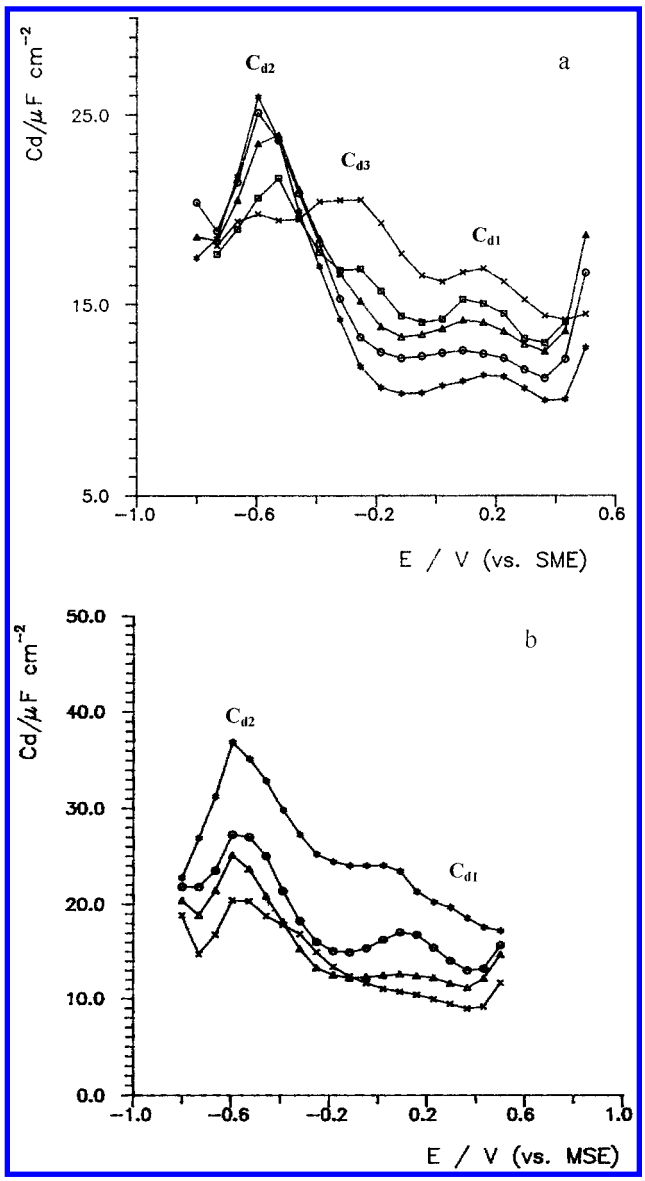


**Figure 5.** (a) $C_d$ vs $E$ plots for a Au electrode ($R = 29$) in 0.1 M $HClO_4$ + $x$ M Pyridine at 25 °C: (×) $x = 0.001$; (□) $x = 0.0025$; (△) $x = 0.005$; (○) $x = 0.0075$; (∗) $x = 0.01$. (b) $C_d$ vs $E$ plots for Au electrodes in 0.1 M $HClO_4$ + 0.01 M pyridine at 25 °C: (∗) $R = 1$; (○) $R = 17$; (△) $R = 32$; (×) $R = 51$.

It should be noted that at $E = -0.7$ V for all curves $C_d$ values tend to approach that obtained in aqueous 0.1 M $HClO_4$.

On the other hand, the influence of $R$ on the $C_d$ vs $E$ plot depends on the solution composition (Figures 5b and 6). In general, these plots exhibit the trend to shift downward as $R$ is increased. But more specifically in the acid solution, the peak value of $C_{d,2}$ decreases and looses sharpness, whereas the value of $C_{d,1}$ remains as a broad peak as $R$ is increased. Conversely, for aqueous 0.1 M $KClO_4$, the $C_d$ vs $E$ plot (Figure 6) shows peaks $C_{d,II}$ and $C_{d,I}$ at 0.3 and −0.5 V, respectively, and $E_{pzc} = -0.28$ V. Likewise, in aqueous 0.1 M $KClO_4$ and with $x = 0.001$, the peak values $C_{d,1}$ at −0.25 V, $C_{d,2}$ at −1.1 V, and $C_{d,3}$ at 0.3 V can be seen (Figure 6). In this case, although the potential difference between the values $C_{d,1}$ and $C_{d,2}$ remains close to 0.7 V, their potential values are shifted −0.060 V pH unit$^{-1}$.

Furthermore, at −1.2 V the $C_d$ value for all curves coincides with that obtained in aqueous 0.1 M $KClO_4$. The shift in the values of $C_{d,1}$ and $C_{d,2}$ with pH suggests that the cationic form of the Py molecule is deprotonated to

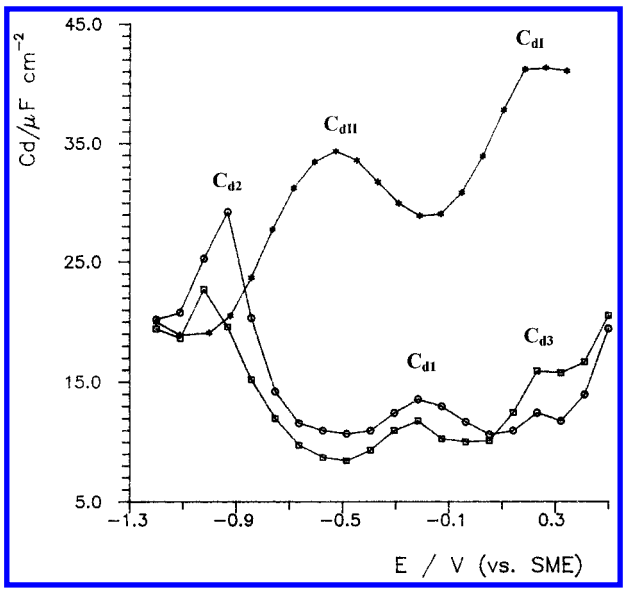


**Figure 6.** $C_d$ vs $E$ plots for Au electrodes in 0.1 M $KClO_4$ [(∗) $R = 1$] and in 0.1 M $KClO_4$ + 0.001 M pyridine [(○) $R = 1$; (□) $R = 17$] at 25 °C.

adsorb on the positively charged Au surface. Peak $C_{d,2}$ has been assigned to Py adsorption, whereas peak $C_{d,1}$ has been related to the reorientation of Py adsorbates.[1,14] Peak $C_{d,3}$ can be identified with peak $C_{d,I}$ in the blanks, which is likely associated with the gold−anion interaction.

**3.3. Chronocoulometry Data.** Values of $\sigma^M$, the charge density related to the adsorption of Py at each $E$, were determined in the following way.[14] The value of $\sigma^b$, the charge density in the blank, was obtained by integration of potentiostatic current transients in the base solution. Similarly, the value of $\sigma$, the charge density resulting from Py-containing solutions, was calculated. Then, $\Delta\sigma = (\sigma^b - \sigma)$, the charge density change due to the presence of Py, was found. Likewise, $\sigma^M$, the absolute value of $\sigma$ in the presence of Py, was calculated by adding $\Delta\sigma$ to the value of $\sigma^s$ resulting from integration with the capacity curve measured in the base solution.

Comparative $\sigma^M$ vs $E$ plots from a Au electrode with $R = 1$ in Py-containing aqueous 0.1 M $HClO_4$ (Figure 7a) show that as the concentration of Py is increased, the value of $\sigma^M$ increases, although all curves intersect at the potential of maximum adsorption $E^M_{ad} \cong 0$ V and $\sigma^M = 10$ $\mu$C cm$^{-2}$.

On the other hand, for $x = 0.01$, the increase in $R$ from 1 to 43 produces no change in the shape of the $\sigma^M$ vs $E$ plots (Figure 7b). The values of $E^M_{ad}$ and $\sigma^M$ remain unchanged although $\sigma^M$ decreases with $R$, approaching the value found for the blank.

The $\sigma^M$ vs $E$ plots obtained for $x = 0.01$ and different values of $R$ (Figure 8) depend on the composition of the base solution. For the $KClO_4$ solutions there is no intersection at a single point in the $\sigma^M$ vs $E$ plots, making, in this case, the estimation of $E^M_{ad}$ and $\sigma^M$ impracticable.

The surface tension ($\gamma$) vs $E$ plots were obtained by integration of the $\sigma^M$ vs $E$ plots,[20] taking arbitrarily $\gamma$ = 400 nN m$^{-1}$ at $E = -0.7$ V for Py-containing aqueous $HClO_4$ solutions and $E = -1.2$ V for Py-containing aqueous $KClO_4$ solutions.

The $\gamma$ vs $E$ plots for $R = 1$ (Figure 9a) shift downward as $x$ is increased, whereas the $\gamma$ vs ln $c$ plots shift upward as $R$ is increased (Figure 9b). A similar effect was observed for aqueous 0.1 M $KClO_4$ base solutions. In this case, the $\gamma$ vs $E$ plots (Figure 10) for $x = 0.01$ show that the increase

(20) Parsons, R.; Peat, R. *J. Electroanal. Chem.* **1981**, *122*, 299.

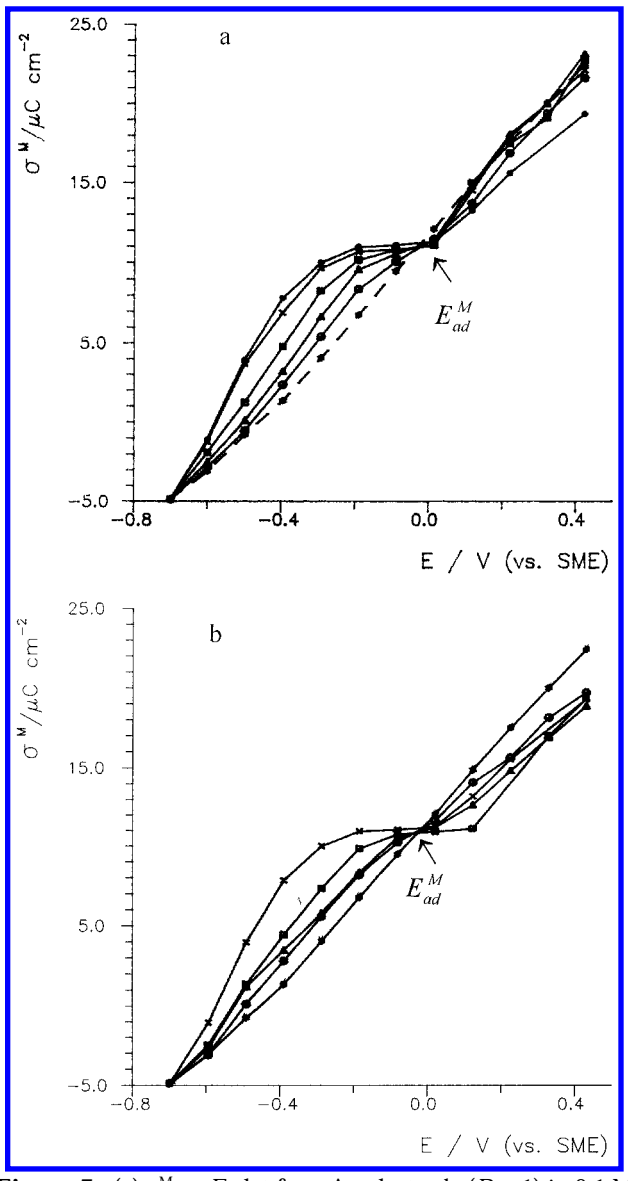


**Figure 7.** (a) $\sigma^M$ vs $E$ plot for a Au electrode ($R = 1$) in 0.1 M $HClO_4$ + $x$ M pyridine: (∗) $x = 0$; (○) $x = 10^{-3}$; (△) $x = 2.5 \times 10^{-3}$; (□) $x = 5 \times 10^{-3}$; (×) $x = 7.5 \times 10^{-3}$; (●) $x = 0.01$. (b) $\sigma^M$ vs $E$ plots for Au electrodes in 0.1 M $HClO_4$ + 0.01 M pyridine at 25 °C: (×) $R = 1$; (□) $R = 10$; (△) $R = 22$; (○) $R = 43$.

in $R$ produces a remarkable increase in $\gamma$. The surface pressure, which is defined as $\Pi = \gamma_0 - \gamma$, where $\gamma_0$ and $\gamma$ are the surface tension in the absence and in the presence of Py in the base solution, was plotted against $E$. For $R = 1$, the $\Pi$ vs $E$ plot shifts downward as $x$ is diminished. Similarly, for $x = 0.01$ M, the $\Pi$ vs $E$ plot also moves downward as $R$ is decreased, a fact which is consistent with a decrease in the specific amount of Py adsorbate on the *we* surface.

The value of $\Gamma$, the relative surface excess of pyridine, was calculated from the equation[20]

$$\Gamma = 1/RT(\partial\gamma/\partial \ln c)_{p,T} \qquad (2)$$

assuming for 0.1 M aqueous base solutions a constant solute activity and taking the activity of Py as the concentration of Py in the solution.

For aqueous 0.1 M $HClO_4$, the $\Gamma$ vs $E$ plots exhibit a parabolic shape with a maximum at $E^M_{ad} \cong 0$ V. As expected for constant $R$, these curves shift downward as $x$ is diminished (Figure 11a), whereas for constant $x$, the same effect can be observed as $R$ is increased (Figure 11b).

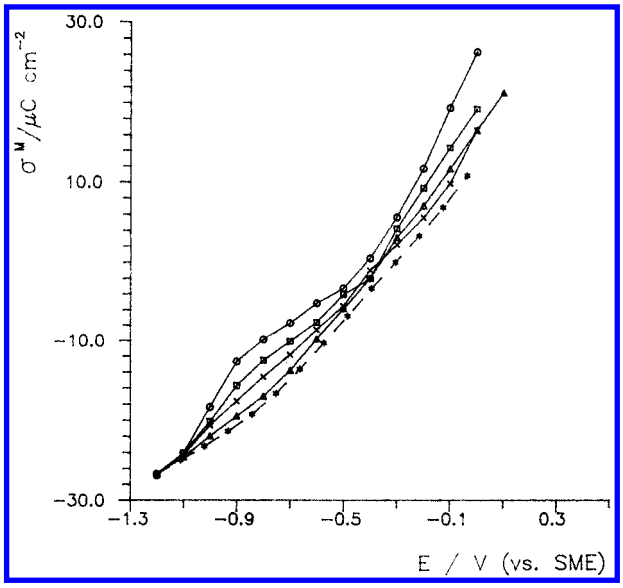


**Figure 8.** $\sigma^M$ vs $E$ plots for Au electrodes in 0.1 M $KClO_4$ + 0.01 M pyridine at 25 °C: (○) $R = 1$; (□) $R = 9$; (×) $R = 17$;(△) $R = 47$.

Conversely, for aqueous 0.1 M $KClO_4$ the same trends as those in the Γ vs $E$ plots can be seen, although no maximum value of Γ can be distinguished in the Γ vs $c$ plot (Figure 12). The extrapolation of the $1/\Gamma$ vs $1/x$ plots for $x \Rightarrow \infty$ yields the value of $\Gamma_s$, the saturation surface excess of Py at the *we*. Values of $\Gamma_s$ in the range $6 \times 10^{-10}$ mol cm$^{-2}$ $\leq \Gamma \leq 8 \times 10^{-2}$ mol cm$^{-2}$ were obtained for both base solutions.

**3.4. STM Imaging.** STM images of stabilized cs-Au electrodes show a typical columnar structure with rounded tops (Figure 13a) and pores with crevices among them. The columnar size distribution yields a mean value of 7 nm. At high resolution the STM images (Figure 13b) reveal small voids and crevices with a cross-section area of about 1−4 nm$^2$, as concluded from the analysis of the image cross sections (Figure 13c). The void profiles, indicated by arrows in Figure 13c, exhibit a width and a depth close to 1.5 nm. It should be noted, however, that there is an intrinsic limitation on determining the smallest void and crevice dimensinos by STM owing to the finite size of the tip itself.[21] Therefore, the presence of smaller features (in size) and larger features (in depth) and those shown cannot be excluded a priori.

## 4. Discussion

**4.1. Adsorption Isotherm of Py on cs-Au Electrodes.** Data on the adsorption of Py on this type of Au electrodes at a constant potential and temperature fit a Frumkin-type adsorption isotherm:[22]

$$\beta c/c_s = [\theta/(1 - \theta)] \exp(-2a\theta) \quad (3)$$

where $\theta = \Gamma/\Gamma_s$, $a$ is the so-called lateral interaction parameter, and $\beta$ is the adsorption coefficient given by

$$\ln \beta/c_s = -\Delta G°/RT \quad (4)$$

where $c$ is the concentration of Py, $\Delta G°$ is the Gibbs energy of adsorption, $T$ is the absolute temperature, $R$ is the universal gas constant, and the concentration of the solvent is $c_s = 55.5$ M.

Equation 3 was tested by plotting $\ln \theta/c(1 - \theta)$ vs $\theta$ plots (Figure 14) at each $E_{ad}$. Data on each set of experimental conditions fit a reasonable straight line whose slope allowed us to estimate the value of $a$, and its extrapolation to $\theta = 0$ yields the value of $\beta$. Finally, from the value of $\beta$ and eq 4, the value of $\Delta G°$ at each $E_{ad}$ can be estimated (Table 1). Values of $\Delta G°$ are referred to the unit mole fraction of Py in the bulk of the solution and the 0.5 Py coverage at the surface as standard states.

For $R = 1$, data assembled in Table 1 for aqueous $HClO_4$ show that $\Delta G° = -23$ kJ/mol and $a = 0.51 \pm 0.03$, irrespective of $E_{ad}$. This value of $\Delta G°$ is close to that recently reported by Lipkowski for 4-cyanopyridine adsorbed perpendicular to the Au(111) surface,[23] although it is lower than the values of $\Delta G°$ reported for essentially the same system.[14] This discrepancy can be understood by taking into account that our isotherms were obtained

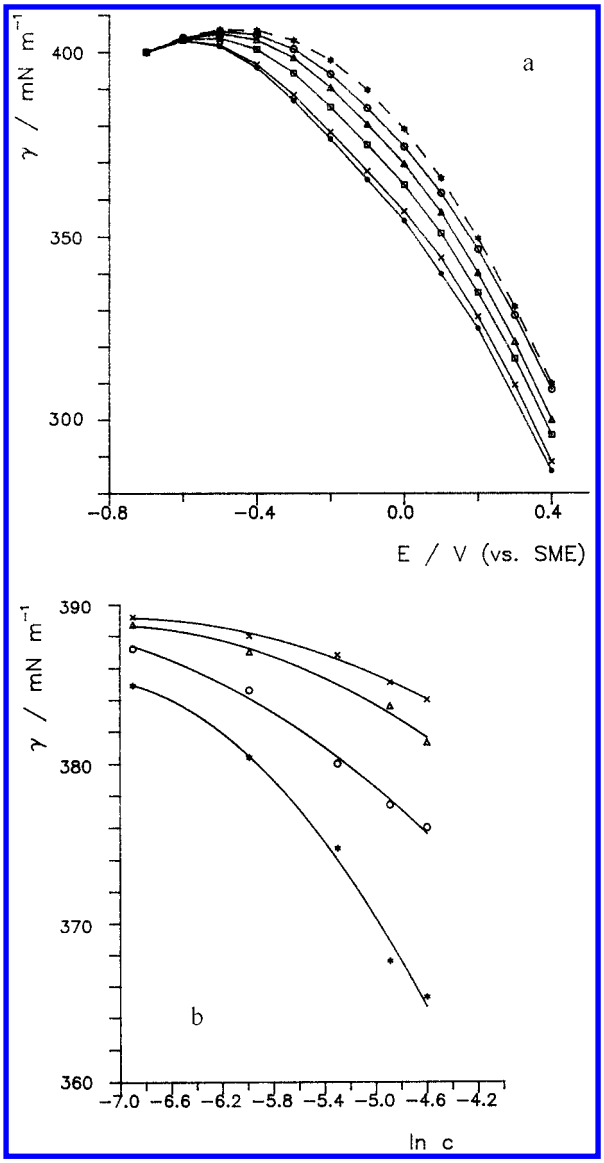


**Figure 9.** (a) $\gamma$ vs $E$ plots for a Au electrode ($R = 1$) in 0.1 M $HClO_4$ + $x$ M pyridine at 25 °C: (∗) $x = 0$; (○) $x = 0.001$; (△) $x = 0.0025$; (□) $x = 0.005$; (×) $x = 0.0075$; (●) $x = 0.01$. (b) $\gamma$ vs ln $c$ plots for Au electrodes in 0.1 M $HClO_4$ + $x$ M pyridine for different values of $R$ at 25 °C: (∗) $R = 1$; (○) $R = 10$; (△) $R = 22$; (×) $R = 43$.

(21) *Artifacts in SPM*; Topometrix Corporation: Santa Barbara, CA, 1994.

(22) Gileadi, E. *Electrosorption*; Plenum Press: New York, 1967. Damaskin, B. B.; Petrii, O. A.; Batrakov, V. V. *Adsorption of Organic Compounds on Electrodes*; Plenum Press: New York, 1971. Damaskin, B. B.; Kazarinov, V. E. In *Comprehensive Treatise of Electrochemistry*; Bockris, J. O'M., Conway, B. E., Yeager, E., Eds.; Plenum Press: New York, 1980; Vol. 1, Chapter 8, p 353 and references therein.

(23) Yang, D. F.; Lipkowski, J. *Russ. J. Electrochem.* **1995**, *31*, 836.

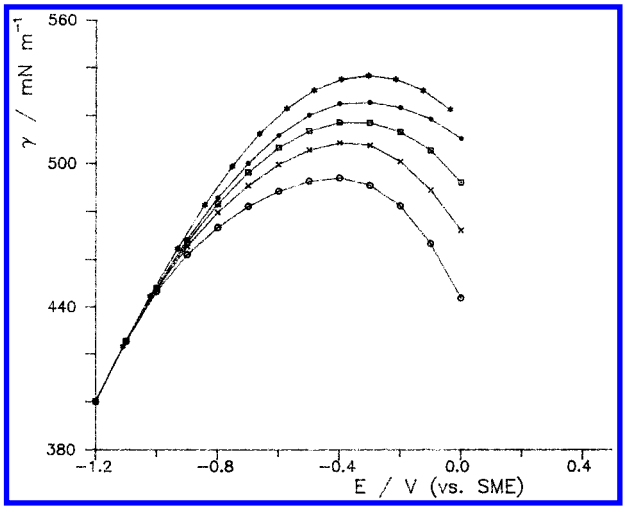


**Figure 10.** $\gamma$ vs $E$ plots for Au electrodes in 0.1 M $KClO_4$ [(∗) $R = 1$] and in 0.1 M $KClO_4$ + 0.01 M pyridine [(○) $R = 1$; (×) $R = 9$; (□) $R = 16$; (●) $R = 28$].

for $E > E_{pzc}$ where the adsorbed molecule lies perpendicular rather than parllel to the surface, as in the case of $E < E_{pzc}$.[1]

The value $\Delta G° = -23$ kJ/mol indicates a weak adsorbate−substrate interaction. Furthermore, the small and positive value of $a$ is consistent with a moderate attractive adsorbate−adsorbate interaction. Similar results are obtained for aqueous $KClO_4$, except that the value of $a$ is always negative, as would be expected for slightly repulsive adsorbate−adsorbate interactions. It should be noted that the $a$ vs $R$ plots (Figure 15) for Py in aqueous $HClO_4$ and $KClO_4$ reproduce qualitatively the adsorption of *o*-phenanthroline in aqueous 0.1 M $HClO_4$ recently reported.[6]

On the other hand, for cs-Au electrodes a constant value of $\Delta G°$ which is slightly lower than that of smooth Au electrodes is found (Table 1), whereas the value of $a$ turns out to increase negatively with $R$. Accordingly, from the value of $a$ it could be concluded that the influence of adsorbate−adsorbate repulsive interactions increases with $R$. However, there is no physical reason to expect an increase in the adsorbate−adsorbate repulsive interactions as the electrode surface becomes rougher. A strong support to this view is that the Γ vs $c$ plots (Figures 11 and 12) can be easily normalized just by taking into account $f$, a surface roughness−dependent correction factor. This factor is an adjustable parameter that takes the value needed to bring the curves closer to that resulting at $E_{ad}^{M}$ for $R = 1$. Thus, when ($\Gamma f$) is plotted vs $E$, all plots tend to approach a single curve (Figure 16) close to that observed for $R = 1$. However, despite the fact that all curves collapse at $E_{ad}^{M}$, a deviation is observed at the minimum values, indicating some dependence of $f$ on $E$. The value of $(1 - f^{-1})$ can be assigned to the fraction of surface sites lost as active adsorption sites for a particular adsorbent; i.e., $f$ reflects the presence of excluded areas (in 2d) or volumes (in 3d) in the substrate, and, as expected, the value of $(1 - f^{-1})$ increases with $R$.

**4.2. Excluded Volume and Adsorbate−Substrate Steric Effect.** The presence of excluded volumes in the rough substrate topography can be related, in principle, to both the size of surface irregularities at the cs-Au electrodes and the specific characteristics of Py adsorbates on Au.

The Py molecule cross section calculated using the MM2 method[24] is either 0.48 or 0.21 $nm^2$ for Py molecules oriented parallel or perpendicular to the substrate,

(24) Allinger, N. L. *J. Am. Chem. Soc.* **1977**, *99*, 8127.

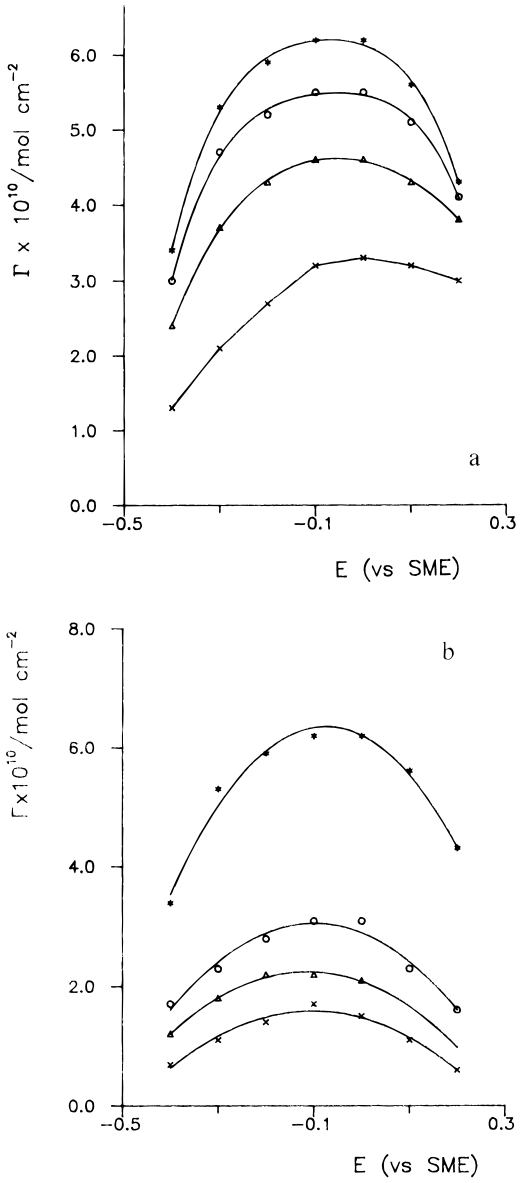


**Figure 11.** (a) Γ vs $E$ plots for a Au electrode ($R = 1$) in 0.1 M $HClO_4$ + $x$M pyridine at 25 °C: (×) $x = 0.0025$; (△) $x = 0.005$; (○) 0.0075; (∗) $x = 0.001$. (b) Γ vs $E$ plots for Au electrodes in 0.1 M $HClO_4$ + 0.01 M pyridine at 25 °C: (∗) $R = 1$; (○) $R = 10$; (△) $R = 22$; (×) $R = 43$.

respectively. For the parallel-oriented molecule $\Gamma_s = 3.4 \times 10^{-10}$ mol $cm^{-2}$, whereas for the perpendicular-oriented molecule $\Gamma_s = 7.9 \times 10^{-10}$ mol $cm^{-2}$, which is in the range $6 \times 10^{-10} \leq \Gamma_s \leq 8 \times 10^{-10}$ mol $cm^{-2}$ obtained experimentally.

From previously published data on the adsorption of Py on smooth Au and single-crystal Au surfaces in the same aqueous solution,[1,14] for $E > E_{pzc}$ V, the Py molecule lies almost perpendicularly oriented with respect to the Au substrate, a situation which appears to be independent of the Au topography, as concluded from data reported in this work. Accordingly, as can be concluded from $\Gamma_s$ data on cs-Au, it is reasonable to assume that the Py adsorbate lies in the same configuration as that of the smooth substrate, this orientation changing only slightly in the ranges of $E$ and $c$ studied in this work. Considering a perpendicular adsorbate configuration, a cross section of 0.21 $nm^2$ is smaller than the value 1−4 $nm^2$, which is the size of the smallest pores detected by STM, and hence, considering only size effects, even the smallest pores would be covered by adsorbates. As this is not precisely the

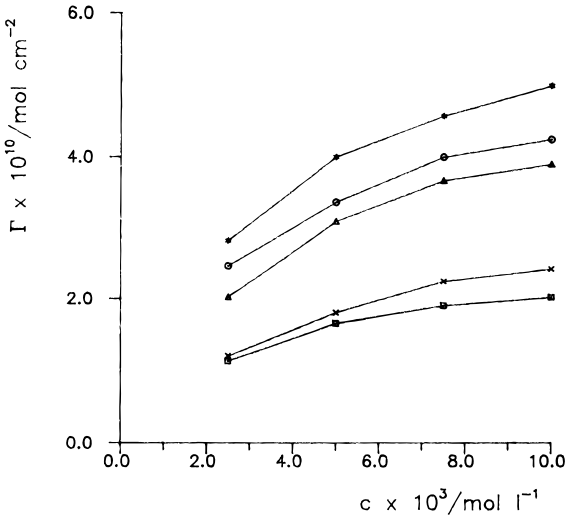


**Figure 12.** Γ vs *c* plots for Au electrodes at $E = -0.4$ V in 0.1 M $KClO_4$ + 0.01 M pyridine: (∗) $R = 1$; (○) $R = 9$; (△) $R = 16$; (×) $R = 28$; (□) $R = 44$.

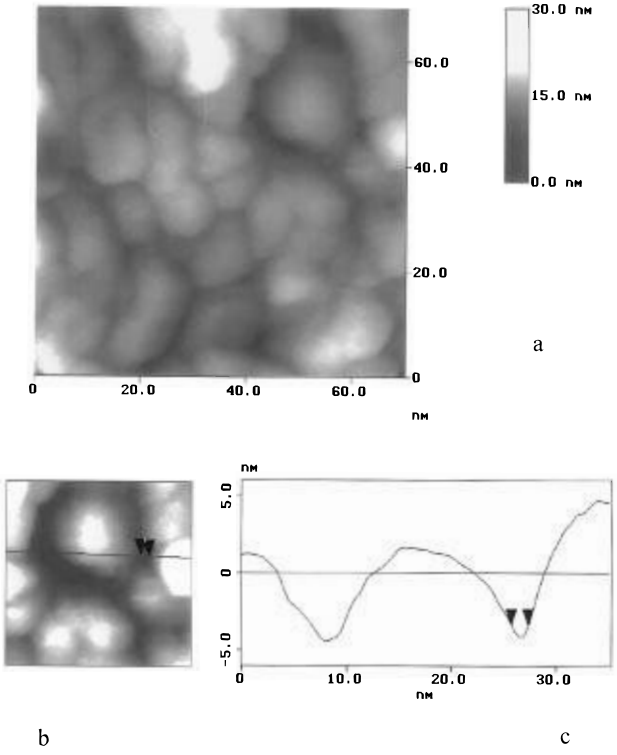


**Figure 13.** In-situ 70 × 70 nm² (a) and 34 × 34 nm² (b) STM images and cross section (c) of a cs-Au electrode ($R = 30$). Arrows indicate a void between columns with a size on the order of $10^{-7}$ cm. The STM images were taken at $E = 0.1$ V in 0.5 M $H_2SO_4$ after cs-Au electrode stabilization in the same solution.

case, simple steric effects, which could provide an explanation for the experimental observations resulting from the adsorption of *o*-phenanthroline on the same electrodes, are not enough for the present case.

**4.3. Excluded Volume and Barrier at Micropore Entrances.** The problem of surface accessibility by adsorbates at micropore regions of an irregular surface, for a micropore size on the order of the adsorbate cross section, implies not only steric effects such as those discussed in the preceding section but also barrier effects at the entrance of the micropores. Therefore, surface barrier effects depend on both the geometry of the pore and the specific properties of adsorbates, and they interfere with the mass transfer of adsorbable species into pores.

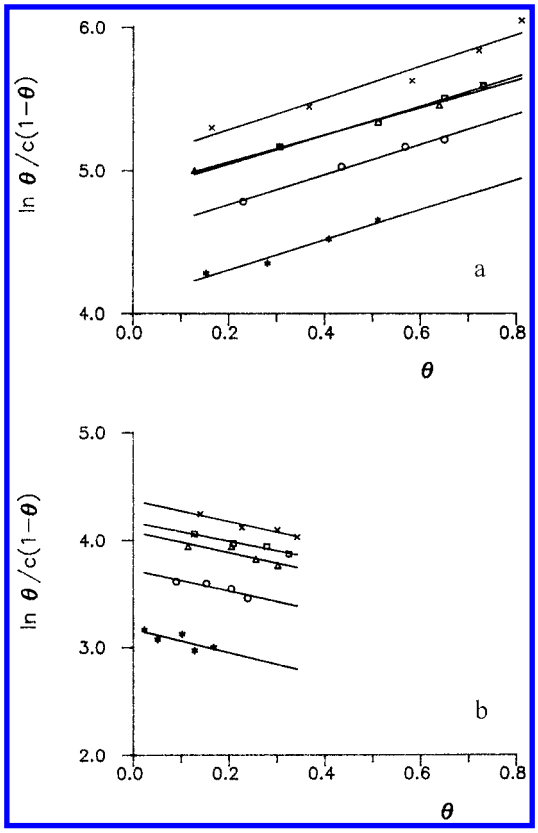


**Figure 14.** (a) Plot of ln $\theta$/c(1 − $\theta$) vs $\theta$ at different $E$ values for a Au electrode ($R = 1$): (∗) $E = -0.4$ V; (○) $E = -0.3$ V; (△) $E = -0.2$ V; (×) $E = -0.1$ V; (□) $E = 0$ V. (b) Plot of ln $\theta/c$(1 − $\theta$) vs $\theta$ at different $E$ values for a Au electrode ($R = 22$): (∗) $E = -0.4$ V; (○) $E = -0.3$ V; (△) $E = -0.2$ V; (×) $E = -0.1$ V; (□) $E = 0$ V.

**Table 1. Values of *a* and Δ*G*° Derived from Eqs 3 and 4 and Data Shown in Figure 13**

| *E*/V | *a* | Δ*G*°/kJ mol$^{-1}$ |
|---|---|---|
| | $R = 1$ | |
| −0.4 | 0.53 | −20.0 |
| −0.3 | 0.53 | −21.2 |
| −0.2 | 0.48 | −22.0 |
| −0.1 | 0.55 | −22.5 |
| 0 | 0.51 | −21.9 |
| | $R = 22$ | |
| −0.4 | −0.53 | −17.8 |
| −0.3 | −0.48 | −19.1 |
| −0.2 | −0.49 | −20.0 |
| −0.1 | −0.50 | −20.8 |
| 0 | −0.45 | −20.3 |

In principle, barrier effects become significant only when the ratio of the adsorbate cross section to the pore entrance size is near unity,[25] which differs from Py adsorption on this type of gold electrode.

The model recently described for gas adsorption on porous electrodes[25] can be reformulated taking into account an enhancement of the barrier effect caused by an adsorbate at the pore entrance. Let us consider a rigid, planar slit entrance of width *d*, formed by adsorbates of effective cross section $d_{cs}$, involving a spherical symmetry for interaction sites (Figure 17). For *d* smaller than $d_{cs}$ adsorbate molecules never penetrate the slit to be located at the inner pore wall. Therefore, these substrate surface domains are excluded areas for adsorption. This situation would become even more complicated on cs-Au for polar molecules. In this case, the arrangement of adsorbates at the slit is presumably different from that at flat domains

(25) Ford, D. M.; Glandt, D. *J. Phys. Chem.* **1995**, *99*, 11543.

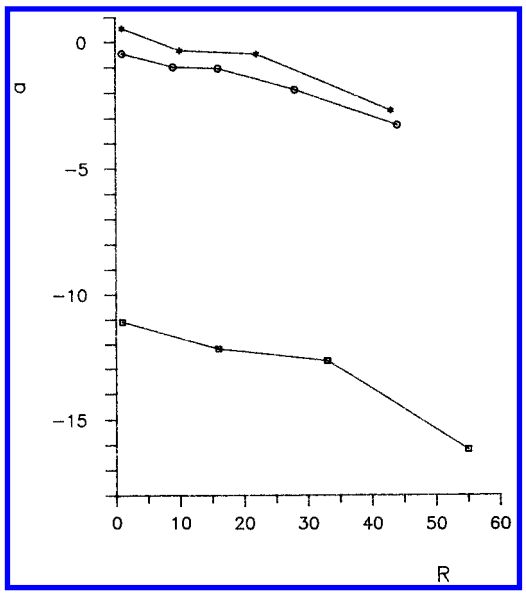


**Figure 15.** Plot of $a$ vs $R$ for the adsorption of different molecules on Au: (∗) 0.1 M 0.1 M $HClO_4$ + pyridine ($E = -0.1$ V); (○) 0.1 M $KClO_4$ + pyridine ($E = -0.4$ V); (□) 0.1 M $HClO_4$ + $o$-phenanthroline ($E = -0.1$ V).

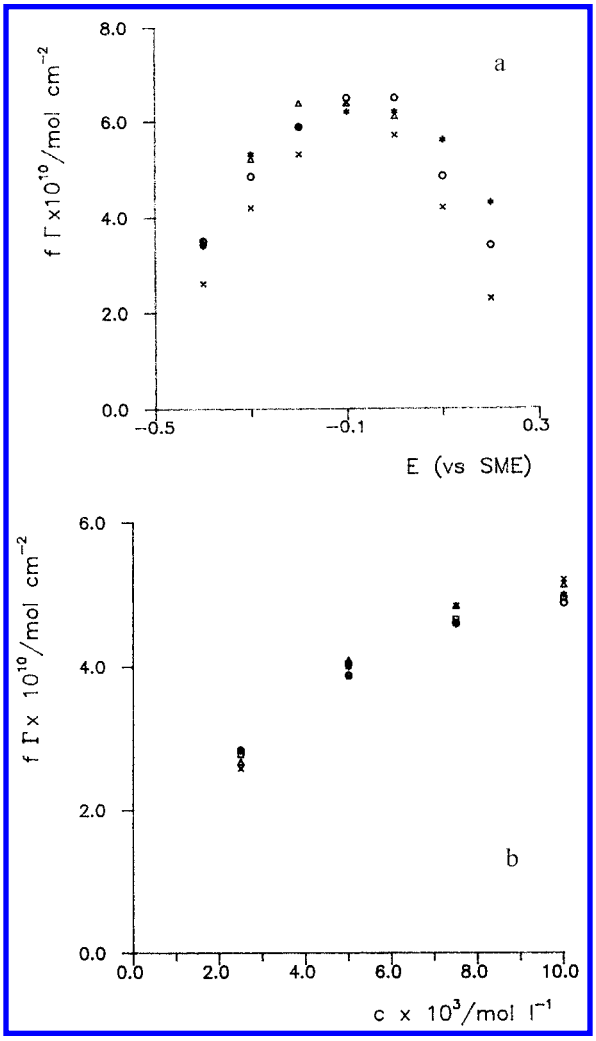


**Figure 16.** (a) Plot of $f\gamma$ vs $E$ in 0.1 M $HClO_4$ + 0.01 M pyridine: (∗) $R = 1$; $f = 1$; (○) $R = 10$, $f = 2.1$; (△) $R = 22$, $f = 2.9$; (×) $R = 43$, $f = 3.8$. (b) Plot of $f\gamma$ vs $c$ for $E = -0.4$ V in 0.1 M $KClO_4$: (∗) $R = 1$, $f = 1$; (○) $R = 9$, $f = 1.15$; (△) $R = 16$, $f = 1.32$; (×) $R = 28$, $f = 2.15$; (□) $R = 44$, $f = 2.45$.

of the substrate, and the overall effect should be further enhanced when the interface has been electrochemically

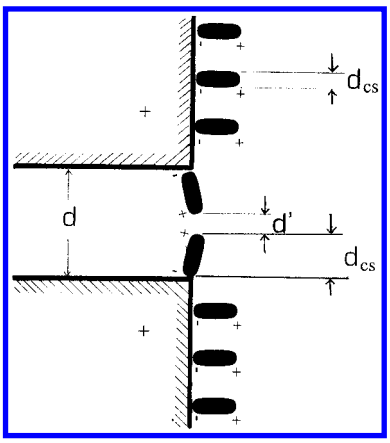


**Figure 17.** Scheme of the barrier effect due to adsorbates at nanometer size pore entrances. The dashed line regions indicate the substrate. Adsorbed pyridine molecules are shown in black. $d$ is the pore size, $d'$ is the effective pore size, and $d_{cs}$ is the molecule cross section.

charged. It should be noted that the potential energy for a noble gas entering the slit has been calculated by considering a Lennard-Jones interaction site model.[26] Attempts to map out the potential energy when dipolar molecules are involved were also made on the basis of semiempirical molecular orbital calculations.[27]

According to the above description for an irregularity 1.5 nm in size (Figure 13), the possibility that two Py adsorbates will be perpendicularly oriented at the pore entrance implies that $d'$, the effective size of the pore, is reduced to $d' = 0.2$ nm or thereabouts. In this case the penetration of other Py molecules into the inner wall of irregularities would be hindered. This fact can explain why the molecular adsorption of Py on cs-Au becomes comparable to that of $o$-phenanthroline under similar conditions. However, it should be noted that the adsorbate could move from the pore entrance to the inner wall by a spillover effect. It means that the barrier could be located at different points of the pore at different times so that the entire pore volume could not be completely blocked for the adsorption. This can occur when weak adsorbate−substrate interactions facilitate adsorbate surface mobility. Then, there may be a trend toward adsorbate spillover on the inner wall of irregularities, the resulting adsorbate structure inside irregularities being altered as compared to that at flat surface domains. Correspondingly, the excluded volume effect should be to some extent reduced but should still be sufficient to induce adsorption/desorption hysteresis loops which have been described as a surface heterogeneity influence on the thermodynamic functions of these processes.[3]

## 5. Conclusions

The molecular adsorption of Py on cs-Au substrates in aqueous $HClO_4$ and $KClO_4$ at 298 K can be explained as a weak localized adsorption. For adsorption potentials more positive than $E_{pzc}$ the Py molecule lies mostly perpendicular to the substrate, as has been demonstrated for smooth Au substrates.

The process can be described by a Frumkin-type adsorption isotherm.

For cs-Au substrates the Frumkin isotherm leads to negative interaction parameters, in contrast to the case

(26) Vlasov, A. I.; Bakaev, A. V.; Dubinin, M. M.; Serpinsky, V. V. *Dokl. Akad. Nauk* **1980**, *215*, 912. Smirnova, L. F.; Bakaev, V. A.; Dubinin, M. M. *Carbon* **1987**, *25*, 599.

(27) Beenakker, J. J. M.; Borman, V. D.; Krylov, Y. S. *Chem. Phys. Lett.* **1995**, *232*, 379.

for smooth Au substrates. The magnitude of the adsorbate−adsorbate repulsive interactions increases as the roughness of the substrate is increased.

The behavior of the interaction parameter for Py adsorption on cs-Au can be related to the presence of small pores and crevices on the substrate surface, as determined by in-situ STM imaging. A correction for this behavior can be made by including an excluded-volume correction factor in the adsorption isotherm.

The excluded volume cannot be accounted for in terms of a simple steric effect. It appears to be related to a barrier effect due to adsorbates at nanometer size pore entrances.

**Acknowledgment.** Financial support was obtained through project PS88-0014 (DGICYT-Spain). R.C.S. and A.J.A. thank CONICET (Argentina) and the Universidad Autónoma de Madrid for their participation in this research project.

LA950937R